


Neutrophil expansion defines an immunoinhibitory peripheral and intratumoral inflammatory milieu in resected non-small cell lung cancer: a descriptive analysis of a prospectively immunoprofiled cohort

Kyle G Mitchell ¹, Lixia Diao,² Tatiana Karpinets,³ Marcelo V Negrao,⁴ Hai T Tran,⁴ Edwin R Parra,⁵ Erin M Corsini,¹ Alexandre Reuben,⁴ Lorenzo Federico,⁶ Chantale Bernatchez,⁶ Hitoshi Dejima,⁵ Alejandro Francisco-Cruz,⁵ Jing Wang,² Mara B Antonoff,¹ Ara A Vaporciyan,¹ Stephen G Swisher,¹ Tina Cascone,⁴ Ignacio I Wistuba,^{4,5} John V Heymach,⁴ Don L Gibbons,^{4,7} Jianjun Zhang,⁴ Cara L Haymaker,⁵ Boris Sepesi¹

To cite: Mitchell KG, Diao L, Karpinets T, *et al*. Neutrophil expansion defines an immunoinhibitory peripheral and intratumoral inflammatory milieu in resected non-small cell lung cancer: a descriptive analysis of a prospectively immunoprofiled cohort. *Journal for ImmunoTherapy of Cancer* 2020;**8**:e000405. doi:10.1136/jitc-2019-000405

► Additional material is published online only. To view please visit the journal online (<http://dx.doi.org/10.1136/jitc-2019-000405>).

CLH and BS contributed equally.

CLH and BS are joint senior authors.

Accepted 30 March 2020



© Author(s) (or their employer(s)) 2020. Re-use permitted under CC BY-NC. No commercial re-use. See rights and permissions. Published by BMJ.

For numbered affiliations see end of article.

Correspondence to

Dr Cara L Haymaker;
CHaymaker@mdanderson.org

Dr Boris Sepesi;
BSepesi@MDAnderson.org

ABSTRACT

Background The biological underpinnings of the prognostic and predictive significance of a relative neutrophilia in patients with non-small lung cancer (NSCLC) are undefined. We sought to comprehensively examine the relationships between circulating and intratumoral neutrophil populations and features of the immune contexture in patients undergoing NSCLC resection.

Methods Preoperative soluble cytokine and angiogenic factors; tumor multiplex immunofluorescence; RNA, whole exome, and T-cell receptor sequencing; and flow cytometry were analyzed for relationships with populations of circulating (from complete blood counts) and intratumoral neutrophils (transcriptional signatures) in a prospectively enrolled resected NSCLC cohort (n=66). In a historical cohort (n=1524), preoperative circulating neutrophil and lymphocyte counts were analyzed for associations with overall survival (OS).

Results Circulating neutrophil populations were positively correlated with increased tumor burden, and surgical tumor resection was followed by a subsequent reduction in peripheral neutrophil counts. Expansion of the circulating neutrophil compartment was associated with increased levels of pro-granulopoietic (IL-1 β , IL-17A, TNF α , IL-6) and T_H2-associated (IL-5, IL-13) cytokines. Tumors with high intratumoral neutrophil burden were marked by a blunted T-cell response characterized by reduced expression of cytotoxic T-cell genes (*CD8A*, *CD8B*, *GZMA*, *GZMB*), decreased CD3⁺CD8⁺ cell infiltration, and diminished expression of IFN γ -related genes. The associations between increased intratumoral neutrophil burden and reduced CD3⁺CD8⁺ infiltration persisted after adjustment for tumor size, histology, mutational burden, and PD-L1 expression. In 1524 patients, elevated preoperative circulating neutrophil count was independently associated

with worse OS (main effect HR 1.82, 95% CI 1.24 to 2.68, p=0.002).

Conclusions Our findings demonstrate that neutrophil expansion reflects protumorigenic and immunosuppressive processes that manifest as worse OS in patients undergoing NSCLC resection. These results justify further investigation of therapeutic strategies targeting neutrophil-associated immune evasion.

INTRODUCTION

Although immune checkpoint inhibitor (ICI) therapy has revolutionized the management of patients with advanced non-small cell lung cancer (NSCLC)¹ and is being investigated in patients with resectable disease,² a significant proportion of patients fail to demonstrate clinically significant responses to therapy. As no therapeutic adjunct that may be used reliably to enhance response to these agents has yet been developed,¹ identification of targetable pathways of tumor immune evasion is of immediate clinical interest.

An elevated pretreatment neutrophil-to-lymphocyte ratio (NLR) has been consistently identified as an adverse prognostic indicator in patients with solid tumors,³ and accruing data attest to its ability to predict diminished therapeutic response to ICIs.^{4,5} However, the biological underpinnings of its utility as a prognostic and possible predictive biomarker are unclear,^{3–5} and whether the association of poor outcomes with elevated NLR reflects the immunological consequences of circulating neutrophil expansion or relative

lymphocyte depletion remains undefined. Elucidation of the basis of this link with poor clinical outcomes might therefore permit investigation of novel targeted therapies. Neutrophils are abundant both in circulation⁶ and in the NSCLC tumor microenvironment⁷ and can expand systemically in response to local inflammatory changes within tumors.^{8,9} Moreover, neutrophils may exhibit local tumor immunosuppressive functions¹⁰ and contribute to metastatic spread.^{11,12} However, despite these mechanistic studies supporting an immunosuppressive and protumorigenic role of neutrophils, direct clinical evidence of an association between neutrophil expansion and impaired antitumor immunity in patients with NSCLC is limited.

In this study, we hypothesized that the reported prognostic significance of elevated NLR reflects immunologic features associated with neutrophil expansion, and that an increased burden of circulating and intratumoral neutrophils is associated with suppression of the antitumor immune response in patients with NSCLC. To that end, we investigated the relationships between circulating and intratumoral neutrophil populations and features of the immune contexture in a prospectively enrolled NSCLC patient cohort (Immunogenomic Profiling of NSCLC (ICON)) and further analyzed the prognostic significance of neutrophil expansion in a large, historical cohort of patients with NSCLC who underwent primary tumor resection in order to elucidate whether relative circulating neutrophil expansion or lymphocyte depletion is more significantly associated with postoperative prognosis. The results of these analyses demonstrated that neutrophil expansion is associated with increased tumor burden, upregulation of progranulocytic and protumorigenic signaling processes, blunted T-cell-mediated antitumor immunity, and poor postoperative clinical prognosis in patients with resectable NSCLC.

METHODS

Study design, population, and treatment

Two cohorts were included for analysis. For translational analyses, we included patients in the multifaceted ICON study at the University of Texas MD Anderson Cancer Center (MDACC), which prospectively enrolled patients with clinical stage IA–IIIA NSCLC prior to resection (2016–2018). Patients in the ICON study were eligible for analysis if they had preoperative systemic cytokine and angiogenic factor (CAF) data available, did not receive any neoadjuvant therapy, and had complete blood count data (absolute neutrophil count and absolute lymphocyte count, both quantified as 10^3 cells/ μ L) available within ≤ 30 days preoperatively (online supplementary figure S1). This preoperative time threshold was selected because it was used in recent investigation of the use of hematologic indices as predictors of therapeutic response to checkpoint inhibitor therapy.¹³

Second, in order to examine the prognostic significance of circulating neutrophil and lymphocyte populations in a larger cohort with a long duration of postoperative

follow-up, we included all patients with clinical stage IA–IIIA NSCLC who underwent resection at our institution between 2000 and 2017. Patients in the historical MDACC cohort were included if they had not received neoadjuvant therapy and had complete blood count data available within ≤ 30 days preoperatively (online supplementary figure S2).¹³ For a subset of these patients ($n=661/1524$, 43%), postoperative complete blood count data (30–180 days postoperatively) were also available. For both cohorts, all tumors were staged according to the seventh edition of the American Joint Committee on Cancer's staging system.¹⁴

Systemic cytokine, chemokine, and angiogenic factor analysis

From consented ICON patients, preoperative blood samples were collected and plasma was separated and stored at -80°C until analysis. For cytokines, chemokines, and angiogenic factors (CAF) analysis, plasma samples were processed and analyzed using multiplexed magnetic bead-based assays (EMD Bioscience Research Reagents, Temecula, CA, USA) as previously published.^{15,16} For all CAF analysis, duplicate samples were analyzed and the mean was reported and used in biomarker analysis. The CAFs included sCD40L, EGF, Eotaxin/CCL11, FGF-2, Flt-3 ligand, Fractalkine, G-CSF, GM-CSF, GRO, IFN- α 2, IFN- γ , IL-1 α , IL-1 β , IL-1ra, IL-2, IL-3, IL-4, IL-5, IL-6, IL-7, IL-8, IL-9, IL-10, IL-12 (p40), IL-12 (p70), IL-13, IL-15, IL-17A, IP-10, MCP-1, MCP-3, MDC (CCL22), MIP-1 α , MIP-1 β , TGF- α , TNF- α , TNF- β , VEGF (MilliporeSigma, Burlington, MA, USA) and sBTLA, sGITR, sHVEM, sIDO, sLAG-3, sPD-1, sPD-L1, sPD-L2, sTim-3, sCD28, sCD80, s4-1BB, sCD27, and sCTLA-4 (ProcartaPlex; ThermoFisher Scientific, Waltham, MA, USA). Analytes that did not pass quality control were disregarded and excluded from analysis. Pairwise correlations between individual CAF analytes and blood count data (neutrophils and lymphocytes) were analyzed using Spearman's correlations, with a false-discovery rate (FDR) threshold of 0.20. Significant correlations with CAF analytes that did not represent deviation from the normal range for the entire cohort were disregarded.

Transcriptomic analysis

RNA sequencing was performed using the NuGEN Ovation RNA-Seq FFPE System v2 (NuGEN, San Carlos, CA, USA) protocol according to manufacturers' instructions. Purified double-stranded cDNA (dscDNA) was generated from 150 ng RNA from fresh frozen tumor specimens and was amplified using both 3' poly(A) selection and random priming. If the dscDNA products were significantly larger than 200 base pairs, shearing was performed in order to optimize sample insert size. Samples were quantified using the NanoDrop ND-3300 spectrophotometer and Invitrogen Quant-iT picogreen DNA quantitation assay (both ThermoFisher Scientific). Then 150 ng of each sample was sheared using the Covaris E220 focused ultrasonicator following the Covaris DNA shearing protocol to obtain final library insert size

of 150–200 bp (both Covaris, Woburn, MA, USA). The fragment sizes were confirmed using Agilent Bioanalyzer High Sensitivity DNA chip (Agilent, Santa Clara, CA, USA) to verify proper shearing. A double-stranded DNA library was created using 100 ng of sheared, dsDNA, preparing the fragments for hybridization onto a flowcell. This was achieved by creating blunt ended fragments and ligating unique adapters to the ends. The ligated products were amplified using 8 cycles of PCR and the resulting libraries were assessed using the Agilent Bioanalyzer High Sensitivity DNA chip to determine successful library construction. A qPCR quantitation was performed on each library to determine the concentration of adapter ligated fragments using an Eppendorf eMotion Real-Time PCR Detection System (Eppendorf, Hauppauge, NY, USA) and a KAPA Library Quant Kit (Kapa Biosystems, Wilmington, MA, USA). Libraries were pooled in equimolar amounts based on the qPCR quantification; a qPCR was run on the pooled libraries to determine the concentration of the pool for bridge amplification. Using the concentration from the Eppendorf qPCR instrument, 15 pM of the library pool was loaded onto a flowcell and amplified by bridge amplification using the Illumina cBot instrument (Illumina, San Diego, CA, USA). A paired-end 76-cycle run was used to sequence the flowcell on a HiSeq 2000 or 2500 Sequencing System (Illumina).

Transcriptome reads were mapped to the reference human genome hg19, and then normalized and quantified as counts using HTSeq-count (HTSeq).¹⁷ The counts were used to prepare inputs for further analysis by other computational tools. The neutrophil cell populations in the tumors were quantified as an abundance score by MCP counter¹⁸ using the transcriptomic markers of neutrophils (*CA4*, *CEACAM3*, *CXCR1*, *CXCR2*, *CYP4F3*, *FCGR3B*, *HAL*, *KCNJ15*, *MEGF9*, *SLC25A37*, *STEAP4*, *TECPR2*, *TLE3*, *TNFRSF10C*, *VNN3*).^{18,19} The activity of the interferon- γ response within the tumor was quantified as a score using the Tumor Immune Dysfunction and Exclusion tool (tide.dfci.harvard.edu)²⁰ using the expression levels of *IFNG*, *STAT1*, *IDO1*, *CXCL10*, *CXCL9*, and *HLA-DRA*. The set of genes represent a known IFN γ signature associated with response to anti-PD-1 blockade.²¹

The *limma* R package (function: *voom*())²² was used to identify genes differentially expressed ($p < 0.05$, $\geq \log_2(1.1)$ [fold-change $\geq 10\%$] gene expression) between tumors with the highest ($n=15$) and lowest ($n=15$) intratumoral neutrophil abundance scores. Gene set enrichment analysis^{23,24} was used to find pathways and hallmark gene sets (within the five databases Canonical Pathways, KEGG, BIOCARTA, PID, and REACTOME) enriched in the set of upregulated and downregulated genes. Transcriptomic data were available for 43 patients in the present study.

Whole-exome sequencing

DNA was extracted from frozen tumor tissue using the QIAamp DNA Mini kit (Qiagen) according to the manufacturer's instructions. Exome capture was performed on 200 ng of genomic DNA per sample based on KAPA

library prep (Kapa Biosystems) using the Agilent SureSelect Human All Exon V4 kit according to the manufacturer's instructions, and paired-end multiplex sequencing of samples was performed on the HiSeq 2500 sequencing platform (Illumina). Blood was used as a normal control. The BWA aligner (bwa-0.7.5a) was applied to map the raw reads to the human hg19 reference genome (UCSC Genome Browser: genome.ucsc.edu).²⁵ Duplicate reads were marked using the Picard (V.1.112, <http://broadinstitute.github.io/picard/>) "MarkDuplicates" module. The Genome Analysis Toolkit (modules "IndelRealigner" and "BaseRecalibrator") was applied to perform insertion/deletion (indel) realignment and base quality recalibration. MuTect and Pindel were applied to each tumor and its matching normal tissue sample to detect somatic single nucleotide variants (SNVs) and small indels.^{26,27} To ensure specificity, the following criteria were applied to filter the detected somatic SNVs and indels: coverage of ≥ 20 reads for tumor and ≥ 10 for normal control; total number of reads supporting the variant ≥ 4 ; MuTect LOD (log odds) score ≥ 6.3 . The allele frequency from the normal sample was less than 0.01%. A population frequency threshold of 1% was used to filter out common variants in the databases of 1000 Genome Project, Exome Aggregation Consortium, and ESP6500. If repetitive sequences were detected within 25 base pairs in the downstream regions of an indel, that indel was discarded. Tumor mutational burden (TMB) was quantified as the total number of non-synonymous mutations per megabase (mut/Mb). TMB was available for 43 ICON patients in this study.

Multiplex immunofluorescence

Multiplex immunofluorescence analysis was performed using methods that have been previously described and validated.²⁸ Briefly, 4- μ m-thick formalin-fixed, paraffin-embedded (FFPE) tumor sections were stained using an automated staining system (BOND-MAX; Leica Microsystems, Wetzlar, Germany) using antibodies against cytokeratin AE1/AE3 (dilution 1:300), PD-L1 (dilution 1:3000), CD3 (dilution 1:100), CD8 (dilution 1:300), and CD68 (dilution 1:450) (all antibodies: Opal 7 kit, catalog no. NEL797001KT; PerkinElmer, Waltham, MA, USA).²⁸ Stained slides were scanned using the Vectra V.3.0 imaging system (PerkinElmer) using fluorescence intervals of 10 λ nm from 420 to 720 nm with normal human tonsil tissue as a calibration control.²⁸ After scanning, five fields (each 0.3345 mm²) were selected within the tumor using the phenochart 1.0.4 viewer (PerkinElmer). A trained pathologist supervised quantification of immune cell densities using InForm image analysis software (PerkinElmer). Marker colocalization was used to identify populations of T lymphocytes (CD3⁺), cytotoxic T lymphocytes (CD3⁺CD8⁺), antigen-experienced T lymphocytes (CD3⁺CD8⁺PD-1⁺), macrophages (CD68⁺), macrophages expressing PD-L1 (CD68⁺PD-L1⁺), malignant cells (MCs, AE1/AE3⁺), and MCs expressing PD-L1 (MCsPD-L1⁺, AE1/AE3⁺PD-L1⁺) in the tumor (epithelial nests) and stromal compartment. Densities of each

colocalized cell population were quantified as the average number of cells per square millimeter.²⁸ Multiplex immunofluorescence data were available for 43 ICON patients in the present study.

Flow cytometry

Fresh tumor tissue was disaggregated using the BD Mediatech System (BD Biosciences) to generate a single cell suspension for subsequent flow cytometry staining. Surface staining was performed in 1×DPBS with 1% bovine serum albumin for 30 min on ice using fluorochrome-conjugated monoclonal antibodies against CD3 (PE-Cy7, Clone UCHT1, Cat. No. 563423; BD Biosciences), CD8 (APC-Cy7, Clone RPA-T8, Cat. No. 557760; BD Biosciences), and TIM3 (APC, Clone F38-2E2 Cat. No. 17-3109-42; eBioscience). Following surface staining, cells were fixed and permeabilized using the BD Cytotfix/Cytoperm solution (Cat. No. 554722; BD Biosciences) according to manufacturer's instructions, and intracellular staining performed in BD Perm/Wash buffer (554723; BD Biosciences) using Perforin (FITC, Clone dG9, Cat. No. 11-9994-42; eBioscience), Granzyme B (V450, Clone GB11, Cat. No. 561151; BD Biosciences), and Interferon- γ (PE, Clone B27, Cat. No. 559327; BD Biosciences) anti-human antibodies. Samples were acquired using the BD FACSCanto II and analyzed using FlowJo Software V.10.5.3 (Tree Star). Dead cells were stained using AQUA Live/Dead fixable dye (Cat. No. L34957; Invitrogen) and excluded from the analysis. A representative dot plot of the flow gating strategy is provided in online supplementary figure S3. Flow cytometric data were available for a subset of ICON patients (n=19).

T-Cell receptor sequencing

Sequencing of the CDR3 region of the T-cell receptor (TCR) β chain was performed using the ImmunoSEQ Assay (Adaptive Biotechnologies, Seattle, WA, USA) according to methods that have been previously described.²⁹ DNA was extracted from freshly resected tumor tissues; following DNA amplification and sequence filtering, TCR clonality, TCR richness, and T-cell density were quantified for each tumor.^{29–31} Analysis was performed using the Analyzer platform (Adaptive Biotechnologies). TCR sequencing data were available for 43 ICON patients included in the present study.

Outcome definitions and statistical analyses

Pairwise associations between continuous variables were analyzed using Spearman's correlations. Associations between tumor neutrophil populations, variables defined a priori to be of interest (histology, PD-L1 expression, TMB, and tumor size), and CD3⁺CD8⁺ cell densities in the tumor and stromal compartments were analyzed using multivariable linear regression; model fitting was guided by Akaike's Information Criterion (AIC).³² Multivariable linear regression analyses of the associations between circulating neutrophil populations and tumor size, pathologic stage, sex, histology, and smoking status were

performed using the same model fitting criteria. Overall survival (OS) was defined as the time from tumor resection until death; patients alive at the end of the study period were censored at the date of last follow-up. Recurrence-free survival (RFS) was defined as the time from resection until disease recurrence or death; those without an RFS event at the time of analysis were censored. Survival times were estimated using the Kaplan-Meier method and differences between groups were analyzed using the log-rank test. In the historical MDACC cohort, univariable Cox proportional-hazards analyses were performed to examine associations between circulating neutrophil and lymphocyte counts, clinicopathologic and treatment characteristics, and postoperative OS. For categorical variables with multiple (>2) levels, binning of subgroups with similar OS was performed, when applicable, after visual inspection of Kaplan-Meier survival curves. Multivariable analysis was performed using variables with p value <0.10 on univariable analysis and those deemed a priori to be of clinical significance (histology and stage), with final model selection guided by minimization of AIC.³² Given the short postoperative follow-up duration (23.9 months, IQR 18.0–28.1 months) and few events (9/66 (14%) deaths; 20/66 (30%) RFS events) at the time of analysis, only exploratory Kaplan-Meier survival analyses were conducted in the ICON cohort. All analyses were performed using R³³ and the threshold for statistical significance was defined as a two-tailed p value <0.05.

RESULTS

Characteristics of the patient cohorts included in the present study

Of the 150 patients enrolled in the ICON study, 66 patients undergoing primary NSCLC resection met inclusion criteria (online supplementary figure S1); the majority of the included patients had adenocarcinoma (47, 71%) and pathologic stage I disease (30, 46%) (online supplementary table S1). Because we also sought to investigate whether the burden of circulating neutrophils has prognostic value while controlling for relevant patient, tumor, and treatment characteristics, we further examined a historical cohort of 1524 patients with NSCLC who underwent curative-intent resection at our institution (online supplementary figure S1). Similar to the ICON cohort, the majority of patients in the historical MDACC cohort had adenocarcinoma and pathologic stage I tumors (online supplementary table S2).

Circulating neutrophil expansion is associated with increased tumor burden and a proinflammatory systemic cytokine profile in patients with NSCLC

Because prior mechanistic studies demonstrated that tumors directly promote neutrophil expansion,^{8 34} we first asked whether circulating neutrophil counts reflect tumor burden in patients with NSCLC. In the ICON cohort, we found that preoperative peripheral neutrophil count was positively correlated with pathologic tumor size

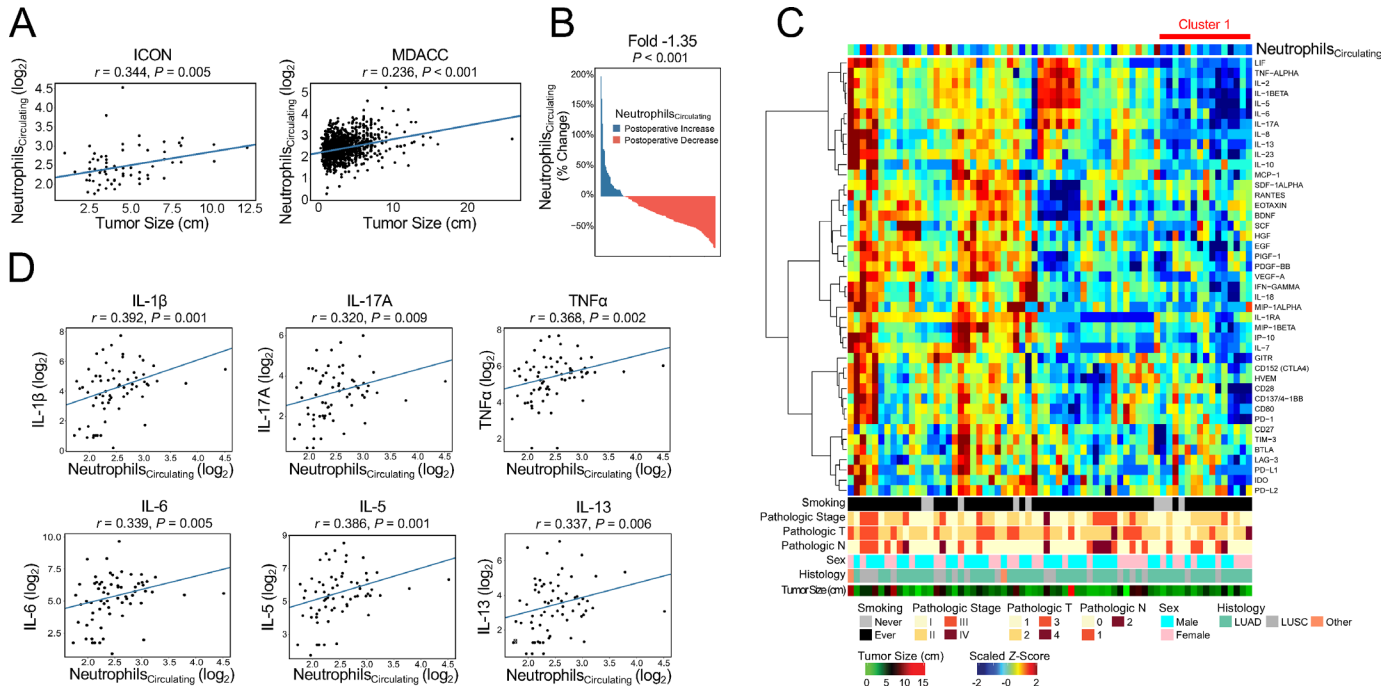


Figure 1 Circulating neutrophil expansion is associated with increased tumor burden and a proinflammatory systemic cytokine profile in patients with resectable non-small cell lung cancer (NSCLC). (A) Pairwise correlations between pathologic tumor size and circulating neutrophil counts in the ICON (left panel, $n=66$) and historical MDACC cohort (right panel, $n=1524$). Values provided are Spearman correlation coefficients. (B) Waterfall plot depicting reduction in circulating neutrophil counts (quantified as percent change from preoperative (≤ 30 days prior to resection) to postoperative (30–180 days following resection)) following surgical resection of NSCLC tumors among the historical MDACC patients with the highest (top quartile) preoperative neutrophil counts ($n=166$ of 661 patients with postoperative complete blood counts available). Fold was calculated using \log_2 -transformed circulating neutrophil counts for this subset of the historical MDACC cohort ($n=166/661$); the p value was calculated using a paired t-test. (C) Unsupervised hierarchical clustering of patients in the ICON cohort according to levels of preoperative soluble cytokine and angiogenic factors (CAF) ($n=66$). Cluster 1 is denoted by the horizontal red bar. (D) Pairwise correlations between preoperative circulating neutrophil counts and levels of soluble CAF analytes ($n=66$). Values provided are Spearman correlation coefficients. In (A) and (D), absolute circulating neutrophil counts (10^3 cells/ μ L) are depicted as \log_2 -transformed values. A two-tailed p value < 0.05 was used to determine statistical significance for all analyses. For (C) and (D), CAF analytes that did not meet quality control measures were disregarded and not included in the analyses.

(figure 1A, left panel), whereas preoperative absolute peripheral lymphocyte count was not (online supplementary figure S4A). We next sought to validate these findings in the historical MDACC cohort, which confirmed the presence of a positive correlation between tumor size and burden of circulating neutrophils (figure 1A, right panel), without a statistically significant association between tumor size and lymphocyte counts (online supplementary figure S4B). Further confirming this relationship between increased tumor size and circulating neutrophil expansion, multivariable regression analyses demonstrated independent associations between tumor size and peripheral neutrophil counts in both the ICON ($p=0.009$, online supplementary table S3) and historical MDACC ($p<0.001$, online supplementary table S4) cohorts after adjusting for sex, histology, stage, and smoking status. Consistent with preclinical work demonstrating that tumor extirpation results in contraction of the neutrophil compartment,⁸ we identified a reduction in peripheral neutrophil counts from preoperative levels to postoperative levels following lung cancer resection (online supplementary figure S4C). The magnitude of

this reduction in circulating neutrophil counts was largest among the patients with the greatest neutrophil expansion (top quartile of preoperative neutrophil count, figure 1B, online supplementary figure S4C). These results demonstrated that peripheral neutrophil expansion, as quantified by circulating neutrophil counts, is a clinical manifestation of overall tumor burden in patients with NSCLC.

Considering this relationship between elevated tumor burden and increased circulating neutrophils, we next investigated whether peripheral neutrophil expansion is indicative of progranulopoietic changes in the systemic inflammatory milieu. Unsupervised clustering analysis identified a distinct subset of patients (cluster 1, figure 1C) with reduced preoperative neutrophil counts and levels of soluble proinflammatory and immunomodulatory factors (IL-1 β , IL-2, IL-8, IL-10, IL-13, IL-17A, IL-23, LIF, TNF α) (figure 1C). Next, analysis of pairwise correlations revealed that increased circulating neutrophil burden was positively associated with increased soluble IL-1 β , TNF α , and IL-17A, which together contribute to a tumor-instigated signaling pathway that culminates

in G-CSF production and neutrophil expansion^{6 8 34 35} (figure 1D, top row panels). In addition, we identified increased levels of IL-6, which induces neutrophil polarization to a protumorigenic phenotype^{36 37} (figure 1D, bottom left panel), and factors consistent with a T_H2 secretory profile (IL-5, IL-13; figure 1D, bottom center and bottom right panels) among patients with increased circulating neutrophil counts. The magnitude of correlation between circulating neutrophil counts and soluble IL-1 β was the greatest of the examined CAF ($r=0.392$; figure 1D, top left panel). In contrast, absolute lymphocyte count was not associated with statistically significant changes in the levels of any of the examined CAF analytes after accounting for multiple comparisons. We next asked whether the progranulopoietic and protumorigenic processes associated with neutrophil expansion were also associated with suppression of the local T-cell antitumor response. We found that elevated soluble IL-17A was correlated with increased intratumoral presence of $CD8^+TIM3^+$ cells ($r=0.623$, $p=0.042$, online supplementary figure S5) and that circulating neutrophils were inversely correlated with intratumoral T-cell density as quantified by TCR sequencing, although the latter association did not reach statistical significance ($r=-0.265$,

$p=0.086$, online supplementary figure S6). Considered together, these results revealed that elevation in circulating neutrophil populations reflects a progranulopoietic systemic inflammatory milieu and pointed toward processes favoring protumorigenic neutrophil polarization and impaired antitumor immunity.

Elevated intratumoral neutrophil burden is associated with a blunted antitumor T-cell response

We next examined whether intratumoral neutrophil burden, rather than signaling via soluble CAF, was associated with aberrations in features of the immune contexture of the tumor microenvironment. Analysis of genes differentially expressed between tumors with high and low intratumoral neutrophil abundance scores identified downregulation of 274 and upregulation of 96 individual genes among patients with elevated intratumoral neutrophil populations (figure 2A). Mirroring the association between elevated soluble IL-17A and neutrophil expansion in circulation, we also noted upregulation of *RORC*, which regulates IL-17-producing lymphocytes,^{38 39} in tumors with the greatest neutrophil burden (figure 2B). We identified reduced expression of *CD3D* (figure 2C, left panel) and *CD247* (figure 2C, right panel), which encode

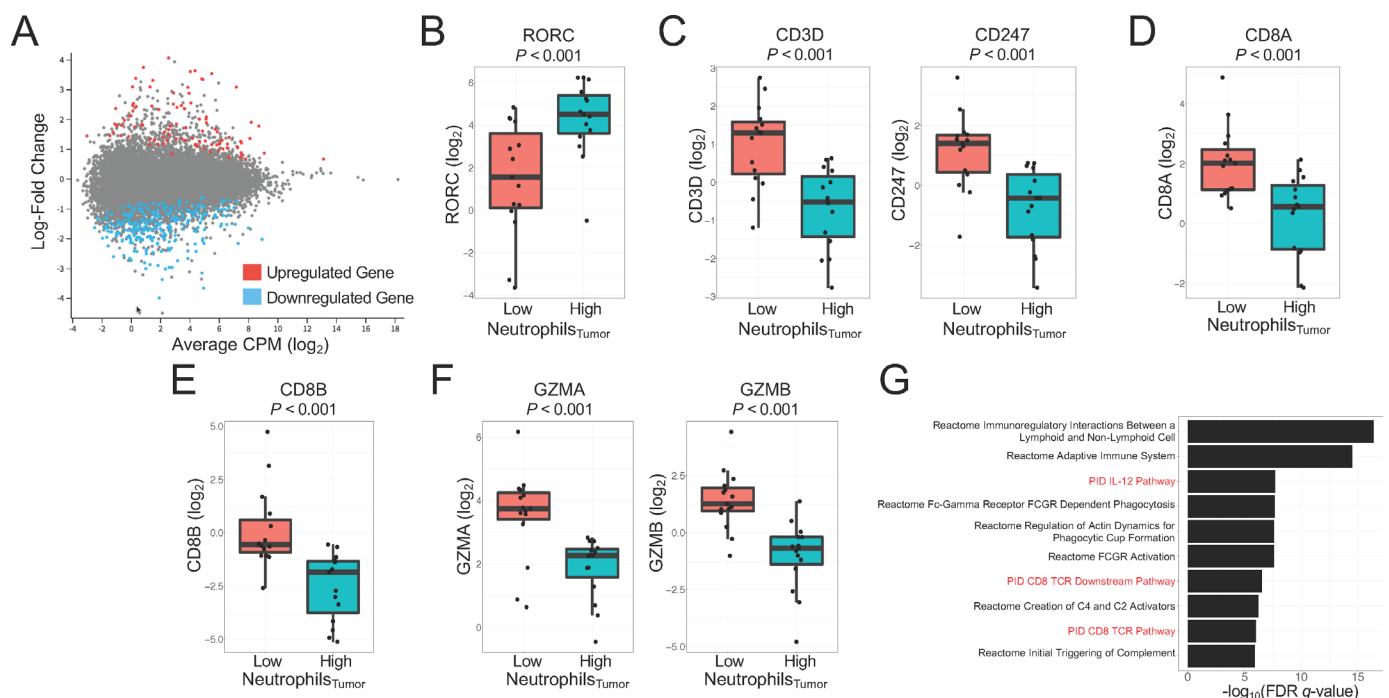


Figure 2 Neutrophil-rich non-small cell lung cancer (NSCLC) tumors are marked by transcriptomic features of a diminished antitumor T-cell response (ICON cohort, $n=43$). (A) Analysis of differentially expressed genes identified downregulation of 274 genes (blue) and upregulation of 96 genes (red) among tumors with the greatest intratumoral neutrophil abundance ($n=15/43$) vs those with the lowest neutrophil populations ($n=15/43$). Intratumoral neutrophil population abundance was determined from the expression of neutrophil transcriptomic markers. (B) NSCLCs with high intratumoral neutrophil burden had upregulated expression of *RORC*, a regulator of IL-17-producing lymphocytes. These tumors were also characterized by reduced expression of genes encoding components of the T-cell receptor complex (*CD3D* and *CD247*, C left and right panels), as well as diminished expression of genes associated with cytotoxic T cells (*CD8A*, D; *CD8B*, E; *GZMA* and *GZMB*, F left and right panels). (G) Gene set enrichment analysis identified downregulation of signaling pathways associated with T-cell activation and effector function (red text) among tumors with increased intratumoral neutrophil burden. The 10 most dysregulated pathways according to $-\log_{10}(\text{FDR } q\text{-value})$ are shown; all were downregulated. CPM, counts per million. A two-tailed p value <0.05 was used to determine statistical significance.

components of the TCR complex (CD3 δ and CD3 ζ , respectively), among tumors with high intratumoral neutrophil abundances. Elevated intratumoral neutrophil burden was further correlated with decreased expression of markers of cytotoxic T cells (*CD8A* (figure 2D), *CD8B* (figure 2E), *GZMA* (figure 2F, left panel), *GZMB* (figure 2F, right panel)), indicating that neutrophil-rich NSCLC tumors were associated with poor intratumoral T-cell infiltration. Examination of significantly downregulated pathways among tumors with elevated neutrophil populations (figure 2G) suggested impaired innate and adaptive antitumor immunity. Notably, these neutrophil-rich tumors demonstrated downregulation of several pathways associated with T-cell activation and effector functions (*IL-12* and TCR signaling pathways; figure 2G, red text). In aggregate, these results demonstrated that increased intratumoral neutrophil abundance was associated with transcriptomic features of a suppressed antitumor T-cell response in resected NSCLCs.

Noting these findings indicative of reduced cytotoxic T-cell infiltration in neutrophil-rich NSCLC tumors, we sought to validate these results at the protein level by analyzing multiplex immunofluorescence data. Mirroring the relationship between expansion of circulating neutrophils and reduced intratumoral T-cell density, as well as the relationship between increased intratumoral neutrophil burden and reduced expression of cytotoxic T-cell markers, we found that neutrophil-rich NSCLCs had lower densities of CD3 $^+$ and CD3 $^+$ CD8 $^+$ cells in both the tumor and stromal compartments (figure 3A–C).

We next examined whether the relationship between increased intratumoral neutrophil populations and diminished cytotoxic T-cell infiltration was independent of relevant tumor pathologic and molecular features. Critically, the associations between increased intratumoral neutrophil burden and reduced CD3 $^+$ CD8 $^+$ cells persisted after adjustment for tumor size, histology, mutational burden, and PD-L1 expression and was the only

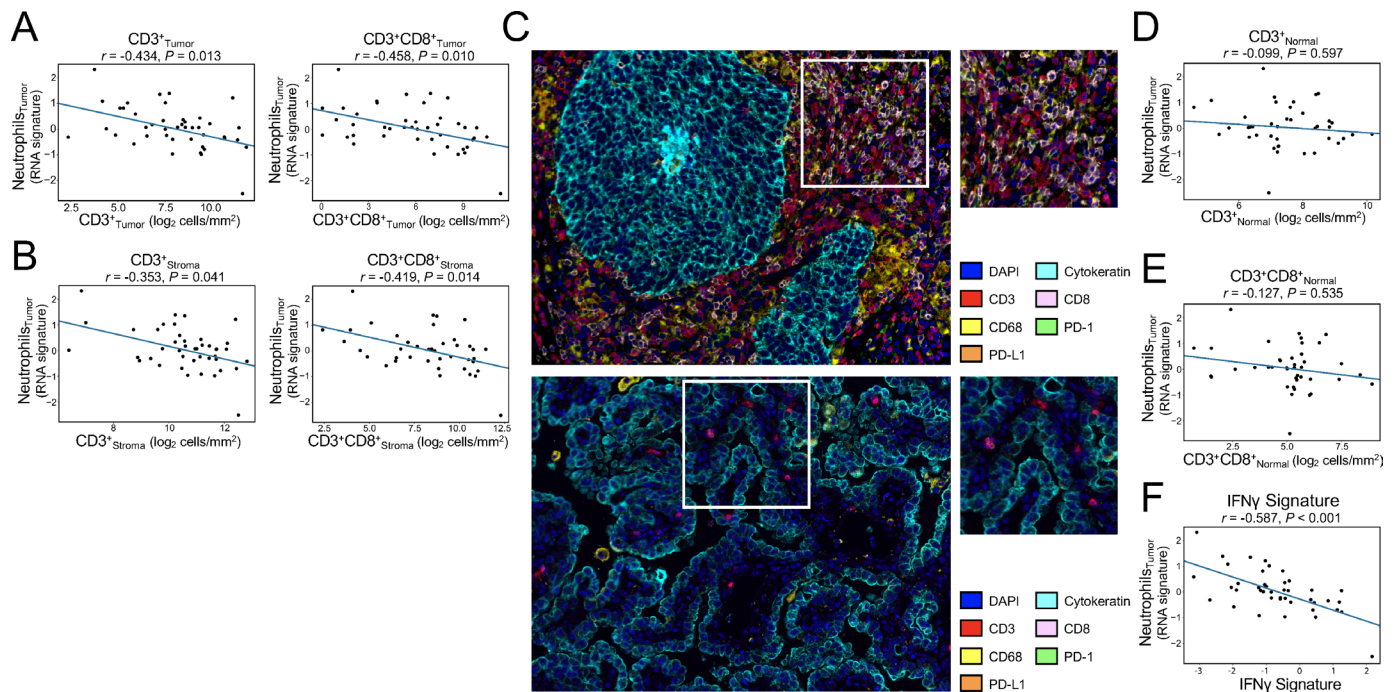


Figure 3 Increased intratumoral neutrophil burden is associated with impaired T-cell trafficking and IFN γ signaling (ICON cohort, $n=43$). (A) Increased neutrophil burden was associated with reduced infiltration of CD3 $^+$ (left panel) and CD3 $^+$ CD8 $^+$ (right panel) cells in the tumor compartment. Intratumoral neutrophil populations were determined according to transcriptomic signatures, and CD3 $^+$ and CD3 $^+$ CD8 $^+$ cell densities were quantified according to multiplex immunofluorescence. (B) Elevated intratumoral neutrophils were associated with reduced CD3 $^+$ (left panel) and CD3 $^+$ CD8 $^+$ (right panel) cell densities in the stromal compartment. (C) Representative multiplex immunofluorescence images of two patients with resected pT2N0 adenocarcinoma. Whereas one patient had low tumor expression of a neutrophil transcriptional signature (abundance score -0.335) and high densities of CD3 $^+$ CD8 $^+$ cells in the tumor (1398.5 cells/mm 2) and stromal (1719.6 cells/mm 2) compartments (top panels), the other had a higher intratumoral neutrophil burden (abundance score 0.783) and low densities of CD3 $^+$ CD8 $^+$ cells (tumor compartment, 1.5 cells/mm 2 ; stromal compartment, 13.9 cells/mm 2) (bottom panels). Left panels are at $\times 20$ magnification; areas outlined in white box are provided in detail in right panels. (D–E) No associations were observed between intratumoral neutrophil burden and CD3 $^+$ (D) or CD3 $^+$ CD8 $^+$ (E) cell densities in normal adjacent lung tissue. (F) Elevated intratumoral neutrophil populations were associated with reduced activity of interferon- γ signature genes (*IFNG*, *STAT1*, *IDO1*, *CXCL10*, *CXCL9*, and *HLA-DRA*). Values provided in (A–B) and (D–F) are Spearman correlation coefficients. P values are adjusted for multiple comparisons according to the Benjamini-Hochberg method. A two-tailed p value < 0.05 was used to determine statistical significance.

feature associated with cytotoxic T-cell densities on multivariable analysis (tumor compartment: $p=0.002$, online supplementary table S5; stromal compartment: $p=0.002$, online supplementary table S6). Interestingly, no relationship was observed between intratumoral neutrophil burden and densities of CD3⁺ or CD3⁺CD8⁺ cells in adjacent normal lung (figure 3D–E), indicating that this neutrophil-associated paucity of T cells was specific to tumor tissue only. We next performed exploratory analyses of intratumoral neutrophil populations according to key oncogenic driver mutations among patients with matched mutation data available and found that no mutation was associated with differences in intratumoral neutrophil populations (*KRAS* (6/39 mutant), $p=0.227$; *EGFR* (4/39), $p=0.333$; *STK11* (7/39), $p=0.199$; *KEAP1* (4/39), $p=0.195$; *ALK* (5/39), $p=0.449$).

Finally, because IFN γ signaling plays a critical role in antitumor cytotoxicity⁴⁰ and has been implicated in clinical response to immune checkpoint inhibitor therapies,^{21–41} we analyzed a published signature of IFN γ response genes (*IFNG*, *STAT1*, *IDO1*, *CXCL10*, *CXCL9*, and *HLA-DRA*).²¹ We identified a strong inverse correlation ($r=-0.587$, $p<0.001$) between increased intratumoral neutrophil abundance and intratumoral activity of IFN γ signature genes (figure 3F). Together, these analyses indicated that an increased burden of circulating and intratumoral neutrophils, as well as systemic processes driving reactive granulopoiesis, are associated with a blunted antitumor T-cell response manifested by impaired intratumoral T-cell trafficking and cytotoxicity in patients with resectable NSCLCs.

Elevated preoperative circulating neutrophil count is associated with poor survival following curative-intent NSCLC resection

Finally, to examine whether these systemic and local immunoinflammatory changes are manifested in clinically relevant outcomes, we retrospectively analyzed a cohort of 1524 patients with NSCLC who underwent curative-intent primary resection at our institution. After a median follow-up duration of 60.7 months (IQR 38.3–94.2 months), there were 533 deaths (35%). Median survival time among the entire cohort was 122.1 months (95% CI 119.5 to 135.9 months; 5-year OS 72.7%). Patients with elevated (top quartile) preoperative neutrophil counts had worse postoperative OS than those with low (bottom quartile) preoperative neutrophil counts (figure 4, $p<0.0001$), suggesting that patients with increased circulating neutrophils represented a patient subgroup at high risk of poor survival. On multivariable analysis, elevated preoperative neutrophil count remained independently associated with an increased hazard of death (main effect adjusted HR 1.82, 95% CI 1.36 to 2.68, $p=0.002$, table 1), whereas preoperative lymphocyte count (main effect adjusted HR 1.50, 95% CI 0.91 to 2.48, $p=0.114$, table 1) was not. Exploratory survival analyses in the ICON cohort demonstrated that elevated preoperative levels of soluble IL-17A (figure 5A, top and bottom panels), IL-6

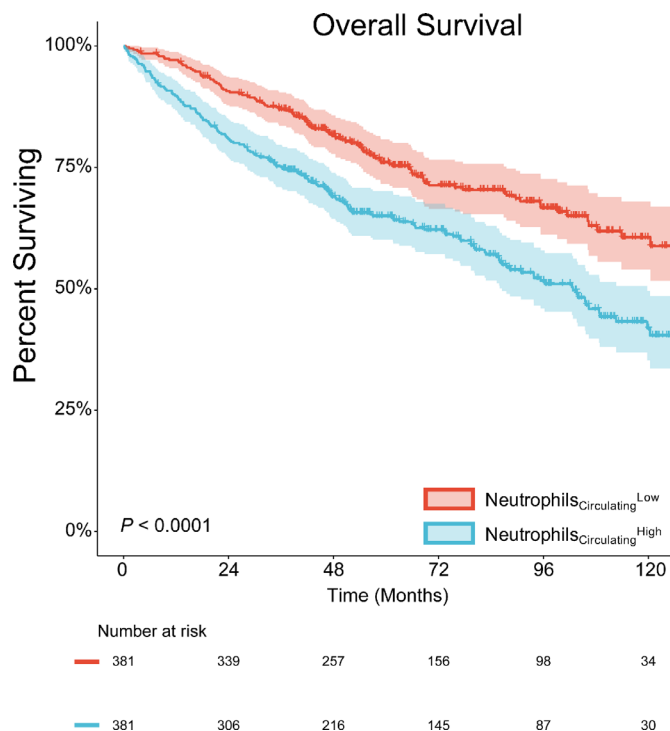


Figure 4 Prognostic significance of preoperative circulating neutrophil expansion in patients undergoing primary resection of non-small cell lung cancer ($n=1524$). Patients in the top quartile of preoperative circulating neutrophil counts (Neutrophils_{Circulating}^{High}, $n=381/1524$) had worse postoperative overall survival than did those in the bottom quartile (Neutrophils_{Circulating}^{Low}, $n=381/1524$). The p value was calculated using a log-rank test; a two-tailed p value <0.05 was used to determine statistical significance.

(figure 5B, top and bottom panels), and IL-13 (online supplementary figure S7A and 7B) were associated with worse postoperative OS and RFS. Considered together, the results of these survival analyses in the historical MDACC and ICON cohorts demonstrated that the proinflammatory and immunosuppressive processes associated with circulating neutrophil expansion are reflected in a clinically significant reduction in postoperative survival outcomes following curative-intent NSCLC resection.

DISCUSSION

In this study, we identified associations between circulating neutrophil expansion with disease burden and protumorigenic systemic signaling in a prospectively enrolled cohort of patients who underwent primary NSCLC resection. Increased intratumoral neutrophil burden was more strongly associated with impaired cytotoxic T-cell trafficking than PD-L1 expression, mutational burden, and histology, and was further associated with reduced T lymphocyte cytotoxicity. In addition, by retrospectively analyzing survival outcomes among a large cohort of patients with NSCLC, we found that expansion of the circulating neutrophil compartment was independently associated with poor postoperative overall survival. Together, our results demonstrate that

Table 1 Multivariable Cox proportional-hazards analysis of associations of clinicopathologic and treatment characteristics with postoperative overall survival in the historical MDACC cohort (n=1524)

Variable	HR	95% CI	P value
Neutrophil count, absolute (10 ³ cells/μL)	1.82	1.24 to 2.68	0.002
Lymphocyte count, absolute (10 ³ cells/μL)	1.50	0.91 to 2.48	0.114
Age, years	1.03	1.02 to 1.04	<0.001
Coronary artery disease	1.30	1.02 to 1.65	0.036
Hypertension	1.22	1.02 to 1.47	0.034
Smoking			
Never	Reference		
Former/current	1.42	1.07 to 1.87	0.014
Zubrod Performance Status			
0	Reference		
1–2	1.31	1.09 to 1.58	0.004
ASA Classification			
1–3	Reference		
4	2.19	1.18 to 4.06	0.013
Histology			
Adenocarcinoma	Reference		
Squamous cell carcinoma	0.99	0.80 to 1.22	0.922
Other	1.19	0.86 to 1.64	0.306
Differentiation			
Low	1.36	1.12 to 1.65	0.002
Moderate	Reference		
High	0.55	0.41 to 0.74	<0.001
Extent of resection			
Sublobar/lobectomy	Reference		
Pneumonectomy	1.54	1.04 to 2.29	0.031
Pathologic stage			
I	Reference		
II	1.74	1.41 to 2.15	<0.001
III–IV	2.14	1.65 to 2.77	<0.001
Pathologic margin			
R0/R1	Reference		
R2	0.35	0.14 to 0.85	0.021
Adjuvant radiotherapy	1.36	1.03 to 1.80	0.029
Neutrophil count×lymphocyte count, interaction	0.77	0.62 to 0.96	0.021

Other variables tested include diabetes mellitus, congestive heart failure, alcohol use, operative approach (thoracoscopic vs thoracotomy), and adjuvant chemotherapy.

neutrophil expansion reflects protumorigenic and immunosuppressive processes that are clinically manifested as worse overall survival in patients with NSCLC, although additional validations and further mechanistic studies are needed to confirm these findings.

IL-1 β signaling induces local inflammatory changes within the tumor microenvironment and is an initiating step in the IL-17A/G-CSF axis that culminates in neutrophil expansion.^{8,42} Here, we identified evidence of upregulated soluble IL-1 β and IL-17A signaling in patients

with NSCLC with expansion of the circulating neutrophil compartment, as well as intratumoral evidence of an increased $\gamma\delta$ T-cell presence among neutrophil-rich NSCLC tumors. In addition, our demonstration of an association between increased soluble IL-17A and increased intratumoral CD8⁺TIM3⁺ cells is supported by upregulation of TIM3 in IL-17A-overexpressing *KRAS*^{Mutant} mice that were also found to be resistant to anti-PD-1 therapy.⁴³ Our findings invite speculation as to whether concomitant targeting of processes associated with systemic

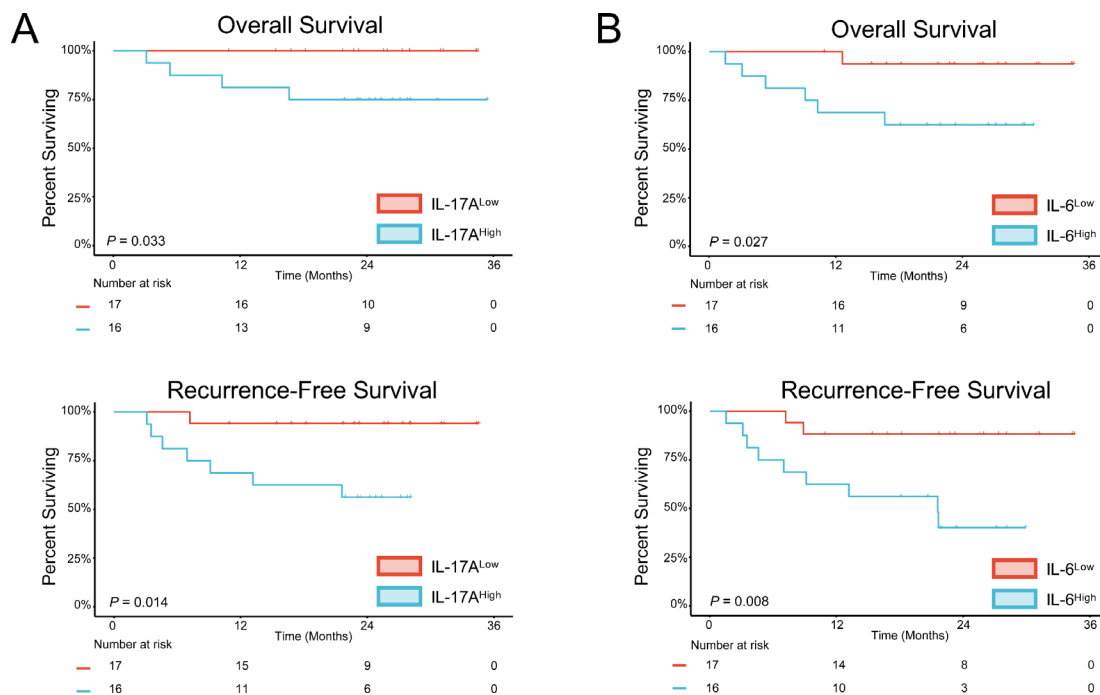


Figure 5 Prognostic significance of soluble cytokines associated with neutrophil expansion in patients with non-small cell lung cancer (ICON cohort, n=66). (A) Reduced overall survival (OS, top panel) and recurrence-free survival (RFS, bottom panel) among patients with elevated (top quartile) vs those with lower (bottom quartile) preoperative levels of IL-17A. (B) Reduced OS (top panel) and RFS (bottom panel) among patients with elevated IL-6. P values were calculated using a log-rank test; a two-tailed p value <0.05 was used to determine statistical significance.

neutrophil expansion and/or intratumoral neutrophil trafficking could be used to enhance the efficacy of cytotoxic or immunotherapeutic agents. Intriguingly, post hoc analysis of a large randomized trial investigating the cardiovascular-protective efficacy of the anti-IL-1 β agent canakinumab identified a marked reduction in incident NSCLC cases and lung cancer-related mortality in patients who received the drug when compared with controls.⁴⁴ Because blockade of IL-1 β in mice resulted in reduced $\gamma\delta$ T-cell production of IL-17A,⁸ and patients receiving IL-1 β or IL-17A inhibitors on phase III trials had moderate reduction in absolute neutrophil counts,^{44 45} the use of anti-IL-1 β or IL-17A agents as a therapeutic adjunct in patients with NSCLC is thus an appealing possibility. Phase III trials of canakinumab anti-IL-1 β monotherapy in the adjuvant setting for resected NSCLCs (NCT03447769), as well as in conjunction with docetaxel in the setting of metastatic disease (NCT03626545), are ongoing.

In this study, we showed that NSCLCs with a high intratumoral neutrophil burden were characterized by a limited antitumor T-cell response and by diminished expression of genes involved in IFN γ signaling. Considering demonstration of improved effect of cisplatin with direct neutrophil targeting in a murine breast cancer model,⁴⁶ as well as the dramatic pathologic response rates identified in preliminary reports of neoadjuvant combination cytotoxic therapy (which can have myelosuppressive effects) and immune checkpoint blockade,⁴⁷ it is plausible that direct suppression of tumor-associated

granulopoiesis might contribute to improved ICI therapeutic efficacy. However, it must be noted that neutrophils play critical roles in protection against external pathogens, and direct neutrophil targeting will require careful consideration of potential infectious toxicity. As a consequence, disruption of dysregulated signaling and granulocyte trafficking pathways may be a more appropriate therapeutic strategy than direct neutrophil inhibition. Preclinical evidence supported targeting of *CXCR2*, the ligands of which are critical mediators of neutrophil trafficking,⁶ as a means of augmenting response to PD-1 blockade in pediatric rhabdomyosarcoma,⁴⁸ and clinical investigation of a *CXCR1/CXCR2* inhibitor in combination with paclitaxel in patients with HER-2^{Negative} breast cancer is underway.⁴⁹ However, data regarding neutrophil targeting agents in patients with NSCLC are sparse, and we propose that therapies directed at suppressing neutrophil expansion and/or intratumoral trafficking be explored as the use of immunotherapies continues to gain wider clinical relevance.

Although the ICON study provides the benefits of comprehensive immunoprofiling and prospective enrollment of a contemporary NSCLC patient cohort, the present work is limited by the relatively small number of patients who met inclusion criteria and the lack of an external validation cohort. The fact that we did not identify correlations between intratumoral neutrophils and any of the driver mutations may be due to type II error. Comprehensive assessment of the relationships between NSCLC genotypes and neutrophil expansion

and intratumoral trafficking requires additional study in larger cohorts. Moreover, given the short follow-up duration and few events at the time of analysis, we were unable to perform robust investigations of the prognostic significance of dysregulated CAF signaling, increased intratumoral neutrophil burden, and impaired T-cell trafficking and function with respect to clinically relevant survival outcomes. However, retrospective analysis of a large institutional cohort of patients with NSCLC who underwent primary resection demonstrated that circulating neutrophil expansion was associated with an increased hazard of death following curative-intent tumor resection, and exploratory stratification of the ICON cohort demonstrated worse postoperative survival outcomes among patients with elevated soluble levels of factors associated with neutrophil expansion. Maturation of outcome data in the ICON cohort will allow for validation of these preliminary findings. In addition, detailed functional characterization of neutrophil activity both in circulation and in tissue requires further study in future NSCLC patient cohorts. Finally, although other investigators have shown alleviation of neutrophil-mediated immunosuppression to result in improved antitumor immunity,⁴³ further studies are needed to examine whether these findings can be used to enhance the clinical efficacy of cytotoxic, targeted, and/or immunotherapeutic agents in the neoadjuvant, adjuvant, and metastatic settings.

In summary, we demonstrate that circulating neutrophil expansion and increased intratumoral neutrophil burden are associated with profound changes in the peripheral and local inflammatory milieu in patients with NSCLC with resectable disease. Although additional studies are needed to validate these findings functionally, our results provide translational evidence that justifies further investigation of agents targeting pathways promoting neutrophil expansion and trafficking as an adjunct to other contemporary therapies in patients with NSCLC.

Author affiliations

¹Thoracic and Cardiovascular Surgery, University of Texas MD Anderson Cancer Center, Houston, Texas, USA

²Bioinformatics and Computational Biology, University of Texas MD Anderson Cancer Center, Houston, Texas, USA

³Genomic Medicine, University of Texas MD Anderson Cancer Center, Houston, Texas, USA

⁴Thoracic/Head and Neck Medical Oncology, University of Texas MD Anderson Cancer Center, Houston, Texas, USA

⁵Translational Molecular Pathology, University of Texas MD Anderson Cancer Center, Houston, Texas, USA

⁶Melanoma Medical Oncology, University of Texas MD Anderson Cancer Center, Houston, Texas, USA

⁷Molecular and Cellular Oncology, University of Texas MD Anderson Cancer Center, Houston, Texas, USA

Acknowledgements This work used the Tissue Biospecimen and Pathology Resource and Research Histopathology Facility at MD Anderson (P30CA016672). This project was supported in part by the Translational Molecular Pathology-Immunoprofiling Lab (TMP-IL) at the Department of Translational Molecular Pathology, The University of Texas MD Anderson Cancer Center. The authors appreciate the assistance of Elliana Young with the Department of Institutional Analytics and Informatics at MD Anderson. We are grateful for the dedication of Lara Lacerda and Emily Roarty; Mei Jiang; our research nurses Mary Ann Gianan

and Craig DeGraaf; consent team May Celestino; blood team Patrice Lawson, Heather Napoleon, Mayra Vasquez, and Eric Prado; and all thoracic OR nurses and anesthesiologists at MD Anderson Cancer Center, without whom this work could not have been completed.

Contributors Conception and design: KGM, CLH, BS. Development of methodology: KGM, LD, TK, JW, JVH, DLG, JZ, CLH, BS. Data acquisition: KGM, MVN, HTT, ERP, EMC, AR, LF, CB, HD, AF-C, MBA, AAV, SGS, TC, IIW, JVH, DLG, JZ, CLH, BS. Analysis and interpretation of data: KGM, LD, TK, MVN, HTT, ERP, EMC, AR, LF, CB, HD, AF-C, JW, MBA, AAV, SGS, TC, IIW, JVH, DLG, JZ, CLH, BS. Writing, review, and revision of the manuscript: KGM, LD, TK, MVN, HTT, ERP, EMC, AR, LF, CB, HD, AF-C, JW, MBA, AAV, SGS, TC, IIW, JVH, DLG, JZ, CLH, BS. Administrative, technical, or material support: HTT, ERP, JW, AAV, SGS, IIW, JVH, DLG, JZ, CLH, BS. Study supervision: CLH, BS. All authors have made material intellectual contributions to this work in accordance with the International Committee of Medical Journal Editors Recommendations.

Funding This work has been supported by generous philanthropic support of the University of Texas MD Anderson Moon Shot Lung Cancer Moon Shots Program, Lung SPORE P50CA070907 and by CCSG P30CA016672; and used the Tissue Biospecimen and Pathology Resource, and the Research Histopathology Facility.

Competing interests DLG has received research funding from AstraZeneca, Janssen, and Takeda and has participated in advisory boards for AstraZeneca and Sanofi. SGS has participated in advisory committees for Ethicon and for the Peter MacCallum Cancer Center. JVH has received research support from AstraZeneca, Bayer, GlaxoSmithKline, and Spectrum; participated in advisory committees for AstraZeneca, Boehringer Ingelheim, Exelixis, Genentech, GlaxoSmithKline, Guardant Health, Hengrui, Lilly, Novartis, Spectrum, EMD Serono, and Synta; and received royalties and/or licensing fees from Spectrum. TC has received speaker's fees from the Society for Immunotherapy of Cancer and Bristol-Myers Squibb and research funding to MD Anderson Cancer Center from Boehringer Ingelheim and Bristol-Myers Squibb. JZ served on advisory board for AstraZeneca and Geneplus and received speaker's fees from BMS, Geneplus, OrigMed, Innovent, grant from Merck, outside the submitted work. BS receives consultation fees from Bristol-Myers Squibb. No potential conflicts of interest are disclosed by the other authors.

Patient consent for publication Not required.

Ethics approval All patients in the Immunogenomic Profiling of Non-Small Cell Lung Cancer (ICON) study gave written informed consent before enrollment, and the study was approved by the MD Anderson Institutional Review Board. The MD Anderson Institutional Review Board approved retrospective analysis of the historical cohort with a waiver of patient informed consent.

Provenance and peer review Not commissioned; externally peer reviewed.

Data availability statement Data are available on reasonable request. Data generated and/or analyzed during this study are available from the corresponding author on reasonable request.

Open access This is an open access article distributed in accordance with the Creative Commons Attribution Non Commercial (CC BY-NC 4.0) license, which permits others to distribute, remix, adapt, build upon this work non-commercially, and license their derivative works on different terms, provided the original work is properly cited, appropriate credit is given, any changes made indicated, and the use is non-commercial. See <http://creativecommons.org/licenses/by-nc/4.0/>.

ORCID iD

Kyle G Mitchell <http://orcid.org/0000-0002-4386-3258>

REFERENCES

- Doroshov DB, Sanmamed MF, Hastings K, *et al*. Immunotherapy in non-small cell lung cancer: facts and hopes. *Clin Cancer Res* 2019;25:4592–602.
- Owen D, Chaff JE. Immunotherapy in surgically resectable non-small cell lung cancer. *J Thorac Dis* 2018;10:S404–11.
- Templeton AJ, McNamara MG, Šeruga B, *et al*. Prognostic role of neutrophil-to-lymphocyte ratio in solid tumors: a systematic review and meta-analysis. *J Natl Cancer Inst* 2014;106:dju124.
- Jiang T, Bai Y, Zhou F, *et al*. Clinical value of neutrophil-to-lymphocyte ratio in patients with non-small-cell lung cancer treated with PD-1/PD-L1 inhibitors. *Lung Cancer* 2019;130:76–83.
- Jiang T, Qiao M, Zhao C, *et al*. Pretreatment neutrophil-to-lymphocyte ratio is associated with outcome of advanced-stage

- cancer patients treated with immunotherapy: a meta-analysis. *Cancer Immunol Immunother* 2018;67:713–27.
- 6 Coffelt SB, Wellenstein MD, de Visser KE. Neutrophils in cancer: neutral no more. *Nat Rev Cancer* 2016;16:431–46.
 - 7 Kargl J, Busch SE, Yang GHY, et al. Neutrophils dominate the immune cell composition in non-small cell lung cancer. *Nat Commun* 2017;8:14381.
 - 8 Coffelt SB, Kersten K, Doornebal CW, et al. IL-17-Producing $\gamma\delta$ T cells and neutrophils conspire to promote breast cancer metastasis. *Nature* 2015;522:345–8.
 - 9 Singel KL, Segal BH. Neutrophils in the tumor microenvironment: trying to heal the wound that cannot heal. *Immunol Rev* 2016;273:329–43.
 - 10 Singel KL, Emmons TR, Khan ANH, et al. Mature neutrophils suppress T cell immunity in ovarian cancer microenvironment. *JCI Insight* 2019;4. doi:10.1172/jci.insight.122311. [Epub ahead of print: 07 Mar 2019].
 - 11 Szczerba BM, Castro-Giner F, Vetter M, et al. Neutrophils escort circulating tumour cells to enable cell cycle progression. *Nature* 2019;566:553–7.
 - 12 Spicer JD, McDonald B, Cools-Lartigue JJ, et al. Neutrophils promote liver metastasis via Mac-1-mediated interactions with circulating tumor cells. *Cancer Res* 2012;72:3919–27.
 - 13 Mezquita L, Auclin E, Ferrara R, et al. Association of the lung immune prognostic index with immune checkpoint inhibitor outcomes in patients with advanced non-small cell lung cancer. *JAMA Oncol* 2018;4:351–7.
 - 14 Goldstraw P, Crowley J, Chansky K, et al. The IASLC lung cancer staging project: proposals for the revision of the TNM stage groupings in the forthcoming (seventh) edition of the TNM classification of malignant tumours. *J Thorac Oncol* 2007;2:706–14.
 - 15 Hanrahan EO, Lin HY, Kim ES, et al. Distinct patterns of cytokine and angiogenic factor modulation and markers of benefit for vandetanib and/or chemotherapy in patients with non-small-cell lung cancer. *J Clin Oncol* 2010;28:193–201.
 - 16 Heymach JV, Shackelford TJ, Tran HT, et al. Effect of low-fat diets on plasma levels of NF- κ B-regulated inflammatory cytokines and angiogenic factors in men with prostate cancer. *Cancer Prev Res* 2011;4:1590–8.
 - 17 Anders S, Pyl PT, Huber W. HTSeq—a Python framework to work with high-throughput sequencing data. *Bioinformatics* 2015;31:166–9.
 - 18 Becht E, Giraldo NA, Lacroix L, et al. Estimating the population abundance of tissue-infiltrating immune and stromal cell populations using gene expression. *Genome Biol* 2016;17:218.
 - 19 Becht EMCPcounter. GitHub Repository, 2016. Available: <https://github.com/ebecht/MCPcounter/blob/master/Signatures/genes.txt> [Accessed March 21, 2020].
 - 20 Jiang P, Gu S, Pan D, et al. Signatures of T cell dysfunction and exclusion predict cancer immunotherapy response. *Nat Med* 2018;24:1550–8.
 - 21 Ayers M, Lunceford J, Nebozhyn M, et al. IFN- γ -related mRNA profile predicts clinical response to PD-1 blockade. *J Clin Invest* 2017;127:2930–40.
 - 22 Law CW, Alhamdoosh M, Su S, et al. Rna-Seq analysis is easy as 1-2-3 with limma, Glimma and edgeR. *F1000Res* 2016;5. doi:10.12688/f1000research.9005.1. [Epub ahead of print: 17 Jun 2016].
 - 23 Subramanian A, Tamayo P, Mootha VK, et al. Gene set enrichment analysis: a knowledge-based approach for interpreting genome-wide expression profiles. *Proc Natl Acad Sci U S A* 2005;102:15545–50.
 - 24 Liberzon A, Subramanian A, Pinchback R, et al. Molecular signatures database (MSigDB) 3.0. *Bioinformatics* 2011;27:1739–40.
 - 25 Gnirke A, Melnikov A, Maguire J, et al. Solution hybrid selection with ultra-long oligonucleotides for massively parallel targeted sequencing. *Nat Biotechnol* 2009;27:182–9.
 - 26 Cibulskis K, Lawrence MS, Carter SL, et al. Sensitive detection of somatic point mutations in impure and heterogeneous cancer samples. *Nat Biotechnol* 2013;31:213–9.
 - 27 Ye K, Schulz MH, Long Q, et al. Pindel: a pattern growth approach to detect break points of large deletions and medium sized insertions from paired-end short reads. *Bioinformatics* 2009;25:2865–71.
 - 28 Parra ER, Uraoka N, Jiang M, et al. Validation of multiplex immunofluorescence panels using multispectral microscopy for immune-profiling of formalin-fixed and paraffin-embedded human tumor tissues. *Sci Rep* 2017;7:13380.
 - 29 Reuben A, Gittelman R, Gao J, et al. TCR repertoire intratumor heterogeneity in localized lung adenocarcinomas: an association with predicted neoantigen heterogeneity and postsurgical recurrence. *Cancer Discov* 2017;7:1088–97.
 - 30 Robins HS, Campregher PV, Srivastava SK, et al. Comprehensive assessment of T-cell receptor beta-chain diversity in alphabeta T cells. *Blood* 2009;114:4099–107.
 - 31 Carlson CS, Emerson RO, Sherwood AM, et al. Using synthetic templates to design an unbiased multiplex PCR assay. *Nat Commun* 2013;4:2680.
 - 32 Akaïke H. Information theory and an extension of the maximum likelihood principle. In: Parzen E, Tanabe K, Kitagawa G, eds. *Selected papers of Hirotugu Akaike*. New York, NY: Springer New York, 1998: 199–213.
 - 33 R Core Team. *R: a language and environment for statistical computing*. Vienna, Austria: R Foundation for Statistical Computing. <http://www.R-project.org/>
 - 34 Casbon A-J, Reynaud D, Park C, et al. Invasive breast cancer reprograms early myeloid differentiation in the bone marrow to generate immunosuppressive neutrophils. *Proc Natl Acad Sci U S A* 2015;112:E566–75.
 - 35 Charles KA, Kulbe H, Soper R, et al. The tumor-promoting actions of TNF-alpha involve TNFR1 and IL-17 in ovarian cancer in mice and humans. *J Clin Invest* 2009;119:3011–23.
 - 36 Yan B, Wei J-J, Yuan Y, et al. IL-6 cooperates with G-CSF to induce protumor function of neutrophils in bone marrow by enhancing STAT3 activation. *J Immunol* 2013;190:5882–93.
 - 37 Walker F, Zhang H-H, Matthews V, et al. IL6/sIL6R complex contributes to emergency granulopoietic responses in G-CSF- and GM-CSF-deficient mice. *Blood* 2008;111:3978–85.
 - 38 Guntermann C, Piaia A, Hamel M-L, et al. Retinoic-acid-orphan-receptor-C inhibition suppresses Th17 cells and induces thymic aberrations. *JCI Insight* 2017;2:e91127.
 - 39 Mielke LA, Liao Y, Clemens EB, et al. Tcf-1 limits the formation of Tc17 cells via repression of the MAF-ROR γ t axis. *J Exp Med* 2019;216:1682–99.
 - 40 Ivashkiv LB. Signalling IFN γ . Ifn γ : signalling, epigenetics and roles in immunity, metabolism, disease and cancer immunotherapy. *Nat Rev Immunol* 2018;18:545–58.
 - 41 Gao J, Shi LZ, Zhao H, et al. Loss of IFN- γ pathway genes in tumor cells as a mechanism of resistance to anti-CTLA-4 therapy. *Cell* 2016;167:397–404.
 - 42 Sutton CE, Lalor SJ, Sweeney CM, et al. Interleukin-1 and IL-23 induce innate IL-17 production from gammadelta T cells, amplifying Th17 responses and autoimmunity. *Immunity* 2009;31:331–41.
 - 43 Akbay EA, Koyama S, Liu Y, et al. Interleukin-17A promotes lung tumor progression through neutrophil attraction to tumor sites and mediating resistance to PD-1 blockade. *J Thorac Oncol* 2017;12:1268–79.
 - 44 Ridker PM, MacFadyen JG, Thuren T, et al. Effect of interleukin-1 β inhibition with canakinumab on incident lung cancer in patients with atherosclerosis: exploratory results from a randomised, double-blind, placebo-controlled trial. *Lancet* 2017;390:1833–42.
 - 45 Gordon KB, Blauvelt A, Papp KA, et al. Phase 3 trials of ixekizumab in moderate-to-severe plaque psoriasis. *N Engl J Med* 2016;375:345–56.
 - 46 Salvagno C, Ciampicotti M, Tuit S, et al. Therapeutic targeting of macrophages enhances chemotherapy efficacy by unleashing type I interferon response. *Nat Cell Biol* 2019;21:511–21.
 - 47 Provencio M, Nadal E, Insa A, et al. Neoadjuvant chemo-immunotherapy for the treatment of stage IIIA resectable non-small-cell lung cancer (NSCLC): a phase II multicenter exploratory study—final data of patients who underwent surgical assessment. *JCO* 2019;37:8509.
 - 48 Highfill SL, Cui Y, Giles AJ, et al. Disruption of CXCR2-mediated MDSC tumor trafficking enhances anti-PD1 efficacy. *Sci Transl Med* 2014;6:237ra67.
 - 49 Schott AF, Goldstein LJ, Cristofanilli M, et al. Phase Ib pilot study to evaluate reparixin in combination with weekly paclitaxel in patients with HER-2-negative metastatic breast cancer. *Clin Cancer Res* 2017;23:5358–65.